Geophysical Research Letters

RESEARCH LETTER
10.1029/2020GL090476

Key Points:

- Three types of iron-containing particles were observed including freshwater diatoms that comprised 38% of particles between 10 and 18 μm
- Aspect ratios increased with particle size suggesting asphericity may aid in transporting supercoarse particles
- Low density and high aspect ratios of diatoms can increase residence times in surface waters and the likelihood of iron dissolution

Supporting Information:

- Supporting Information S1

Correspondence to:
C. J. Gaston,
cgaston@rsmas.miami.edu

Citation:
Barkley, A. E., Olson, N. E., Prospero, J. M., Gatineau, A., Panechou, K., Maynard, N. G., et al. (2021). Atmospheric transport of North African dust-bearing supermicron freshwater diatoms to South America: Implications for iron transport to the equatorial North Atlantic Ocean. *Geophysical Research Letters*, *48*, e2020GL090476. https://doi.org/10.1029/2020GL090476

Received 21 AUG 2020
Accepted 5 JAN 2021

Atmospheric Transport of North African Dust-Bearing Supermicron Freshwater Diatoms to South America: Implications for Iron Transport to the Equatorial North Atlantic Ocean

Anne E. Barkley[1], Nicole E. Olson[2], Joseph M. Prospero[1,3], Alexandre Gatineau[4], Kathy Panechou[4], Nancy G. Maynard[3], Patricia Blackwelder[1,5], Swarup China[6], Andrew P. Ault[2], and Cassandra J. Gaston[1]

[1]Rosenstiel School of Marine and Atmospheric Science, University of Miami, Miami, FL, USA, [2]Department of Chemistry, University of Michigan, Ann Arbor, MI, USA, [3]Cooperative Institute for Marine and Atmospheric Science, Rosenstiel School of Marine and Atmospheric Science, University of Miami, Miami, FL, USA, [4]ATMO-Guyane, Remire-Montjoly Guyane, France, [5]Center for Advanced Microscopy, Department of Chemistry, University of Miami, Miami, FL, USA, [6]Environmental Molecular Sciences Laboratory, Pacific Northwest National Laboratory, Richland, WA, USA

Abstract The equatorial North Atlantic Ocean (NAO) is a nutrient-limited ecosystem that relies on the deposition of long-range transported iron (Fe)-containing aerosols to stimulate primary productivity. Using microscopy, we characterized supermicron and supercoarse mode African aerosols transported to the western NAO in boreal winter/spring. We detected three particle types including African dust, primary biological aerosol particles, and freshwater diatoms (FDs). FDs contained 4% Fe by weight due to surficial dust inclusions that may be susceptible to chemical processing and dissolution. FDs were typically larger than dust particles and comprised 38% of particles between 10 and 18 μm in diameter. The low density, high surface-area-to-volume ratio, and large aspect ratios of FD particles suggest a mechanism by which they can be carried great distances aloft. These same properties likely increase the residence time of FDs in surface waters thereby increasing the time for Fe dissolution and their potential impact on marine biogeochemical cycles.

Plain Language Summary Atmospheric aerosols from Africa are transported by the trade winds to the western equatorial North Atlantic Ocean every winter and spring and can contain nutrients, such as iron (Fe). In this study, we measured the size and composition of supermicron (diameter (d) > 1 μm) aerosols collected at a site on the northeast coast of South America. Using electron microscopy, we found three distinct Fe-containing particle types: mineral dust, freshwater diatoms from African paleolakes, and pollen grains; all three particle types extended into the supercoarse mode (d > 10 μm). Particle asphericity increased with increasing particle size and could explain in part the long-range transport of supercoarse particles. Electron mapping of freshwater diatoms also revealed surficial Fe-rich inclusions. Once deposited in the ocean, the asphericity and light density of freshwater diatom particles likely increases their residence time and therefore, the time for Fe dissolution in the surface ocean compared to dust.

1. Introduction

There is great interest in the atmospheric transport of mineral dust because of the role that associated nutrients such as iron (Fe) play in biogeochemical cycles (Mahowald et al., 2005; Mills et al., 2004; Moore et al., 2013; Okin et al., 2011; Rizzolo et al., 2017). The transport distance of dust is determined in part by the particle size, density, and shape with larger, denser, and more spherical particles predicted to settle more quickly out of the atmosphere (Huang et al., 2020; Mallios et al., 2020). Consequently, particles larger than 5 μm, which includes supercoarse mode particles (diameter > 10 μm), are often ignored in climate studies (Kok et al., 2017; Myriokefalitakis et al., 2018). However, field studies have shown that large particles can be transported far from their source (Betzer et al., 1988; Denjean et al., 2016b; Glaccum & Prospero, 1980; Prospero et al., 1970; Ryder et al., 2019; Weinzierl et al., 2009, 2017). Recently, Adebiyi and Kok (2020) show the need to better characterize the properties and size distribution of supermicron particles because of their

importance to various climate properties. There is relatively little research that has quantified the role of large particles deposited to remote oceans, but recent work suggests that large particles are important (Jickells & Moore, 2015; van der Does et al., 2018; Wang et al., 2015).

African dust is transported to the western equatorial North Atlantic Ocean (NAO) during the boreal winter and spring (Barkley et al., 2019; Prospero et al., 1981, 2020). The equatorial NAO is a nitrogen (N)-limited system, and the atmospheric deposition of Fe stimulates N-fixers that relieve N-limitations, increasing primary productivity and leading to the sequestration of atmospheric carbon dioxide (Mahowald, 2011; Mills et al., 2004; Moore et al., 2013; Okin et al., 2011; van der Does et al., 2016). Dust is thought to be the primary source of Fe delivered to this ecosystem with much of this dust delivered as supermicron particles (Moran-Zuloaga et al., 2018), but other aerosol particle types have also been shown to be important for Fe deposition (Buck et al., 2010; Hamilton et al., 2020; Ito et al., 2019; Scholes & Andreae, 2000; Trapp et al., 2010). Dust has a residence time in the surface ocean on the order of a few weeks with larger particles having shorter residence times than smaller particles, suggesting larger particles may have a limited impact on marine productivity unless they contain forms of Fe that are readily soluble (Gaston, 2020; Jickells & Moore, 2015).

Dust transport during winter and spring occurs primarily in the Saharan Air Layer (SAL), an elevated hot, drier layer of air located at an altitude of approximately 1.5–3 km (Ansmann et al., 2009; Carlson & Prospero, 1972; Chiapello et al., 1995; Prospero et al., 2020; Tsamalis et al., 2013). During transport, dust can mix with clouds, sea-spray aerosol, and sulfur (S)-containing emissions in the marine boundary layer (MBL) (Fraund et al., 2017; Wu et al., 2019). Interactions between dust and trace acidic gases can induce chemical reactions that enhance Fe solubility (Ingall et al., 2018; Paris & Desboeufs, 2013; Paris et al., 2010; Spokes & Jickells, 1995). The size and location of Fe-bearing compounds on aerosols is important with smaller particles and surficial forms of Fe undergoing the most efficient dissolution and chemical reactions (Baker & Jickells, 2006; Gaston, 2020; Journet et al., 2008; McDaniel et al., 2019; Shi et al., 2009). Recent work has shown the presence of surficial Fe nanoparticles attached to larger dust particles that may be an important source of soluble Fe (Lafon et al., 2006; Moskowitz et al., 2016).

In this study, we present measurements of aerosol samples collected at Cayenne, French Guiana, a site located on the North Atlantic coast that is impacted by the long-range transport of African dust (Barkley et al., 2019; Prospero et al., 1981, 2020). Using scanning electron microscopy (SEM), we measured particle size and aspect ratios (ARs; length to width ratios), which is a measure of particle sphericity. Our results show the presence of other types of Fe-containing supermicron particles in addition to mineral dust. Surprisingly, many of these particles were determined to be supercoarse mode in size. Using energy dispersive X-ray spectroscopy (EDX) and elemental mapping, we determined the size and spatial location of Fe inclusions. From these results, we discuss the mechanisms of the transport of supermicron and supercoarse mode Fe-containing particles from Africa and their implications on marine biogeochemical cycles.

2. Materials and Methods

2.1. Sample Collection

Our sampling site is located north of Cayenne, French Guiana (4.92°N, 52.31°W) on a small peninsula at 67 masl. Samples were collected on 20 cm by 25 cm Whatman-41 cellulose filters with an average airflow rate of 0.75 m^3 min^{-1}. Filters are exposed directly to the atmosphere under a Plexiglas "hat"; the cutoff diameter is estimated to be 80–100 μm or greater. We analyzed 13 samples collected between December 15, 2015 and March 31, 2016. Our analysis focuses on supermicron particles, which preferentially deposit near the surface of the filters. These supermicron particles are more easily identified by SEM than submicron particles, which tend to penetrate deeper within the filter prior to being captured. Future work will utilize electron microscopy grids to capture finer particles.

2.2. Air Mass Histories

Air mass back trajectories (AMBTs) were computed using the Hybrid Single Particle Lagrangian Integrated Trajectory (HYSPLIT) model (Rolph et al., 2017; Stein et al., 2015). AMBTs show that air masses originate from North Africa during the boreal winter and spring (Barkley et al., 2019). We also include three AMBT frequency plots shown in the supporting information (SI) Figures S1a–S1c initialized at 500, 1,000, and 2,000 masl, respectively. Each AMBT was run for 240 h at regular intervals of 12 h from December 15, 2015 to March 31, 2016. We emphasize that HYSPLIT cannot be used to determine an exact dust source location because we do not know at what point along the trajectory the dust was injected into the atmosphere and carried to altitudes significant for long-range transport.

2.3. Scanning Electron Microscopy (SEM) and Energy Dispersive X-ray Spectroscopy (EDX)

SEM-EDX analysis yields simultaneous information about the size, morphology, and chemical composition of aerosols. A 1 cm by 1 cm piece of cellulose filter was gently torn with gloved hands and placed on a carbon tab on an aluminum SEM stub for SEM-EDX analysis. The samples were coated with palladium (Pd) in a Cressington-108 Sputter Coater and imaged with a Phillips XL-30/ESEM-FEG at 20 kV and 1.6 nA (Figure 1). An EDX spectrum of a blank filter can be found in Figure S2. The EDX spectra shown in Figure 1 and EDX elemental maps (Figure 2) were obtained with a FEI Helios 650 Nanolab Dualbeam at 20 kV and 0.8–1.6 nA. EDX analysis was performed on a different microscope that was fitted with a light element detector. The corresponding larger field-of-view images corresponding to the spectra in Figure 1 are shown in the SI (Figure S3). Elemental maps provide spatial information regarding individual elements. These maps were analyzed with GENESIS software EDX version 5.10. Each particle analyzed by EDX was magnified to fill the width of the scanning display window (Falkovich et al., 2001).

2.4. Particle Sizing and Aspect Ratios (AR_{perp})

Particles were measured using ImageJ (https://imagej.nih.gov/ij/). The longest dimension was taken as the diameter, d_{max}. Of the 2,206 particles analyzed, 2,153 had a d_{max} greater or equal to 1.0 μm. d_{max} was then converted to projected area diameter, d_{pa}. Of the total particles, 2,102 particles had a d_{pa} greater or equal to 1.0 μm. Aspect ratios (ARs), which provide a measure of particle sphericity, were computed by dividing d_{max} by the width at the largest point that is perpendicular to d_{max}, which hereafter is called AR_{perp} (Huang et al., 2020). More details regarding these calculations can be found in the SI.

3. Results and Discussion

3.1. Transported Fe-Containing Supermicron Particle Types

Three distinct particle types were observed: African dust (Figure 1a), freshwater diatoms (FDs) internally mixed with dust (Figure 1b and 1c), and primary biological aerosol particles (PBAPs) (Figure 1d). To the right of each representative SEM image is an EDX spectrum depicting the elemental composition of each particle type. Particles were categorized by morphology, size, and chemical composition and were similar to supermicron particles previously observed when African dust is transported to South America (Artaxo et al., 1988; Moran-Zuloaga et al., 2018; Pöschl et al., 2010; Rizzolo et al., 2017; Worobiec et al., 2007; Wu et al., 2019).

Dust comprised 95.5% of all particles analyzed by number (Figure 1a). These particles contained a large fraction of aluminum (Al) and silicon (Si), likely from aluminosilicate minerals, that were incorporated within every dust particle except quartz particles, which were composed entirely of Si and oxygen (O) and few in number (<1%). Additional elements detected include magnesium (Mg), which was found in 16% of particles. Calcium (Ca) was found in 29% of particles. Chlorine (Cl) was found in 11% of all particles and sodium (Na) was found in 20%. Cl and Na in dust particles is likely the result of sea-spray coagulation with dust during transport in the MBL. However, small amounts of halite are found in North African soils, which could contribute some Na and Cl to our samples (Scheuvens et al., 2013). Previous work on particles

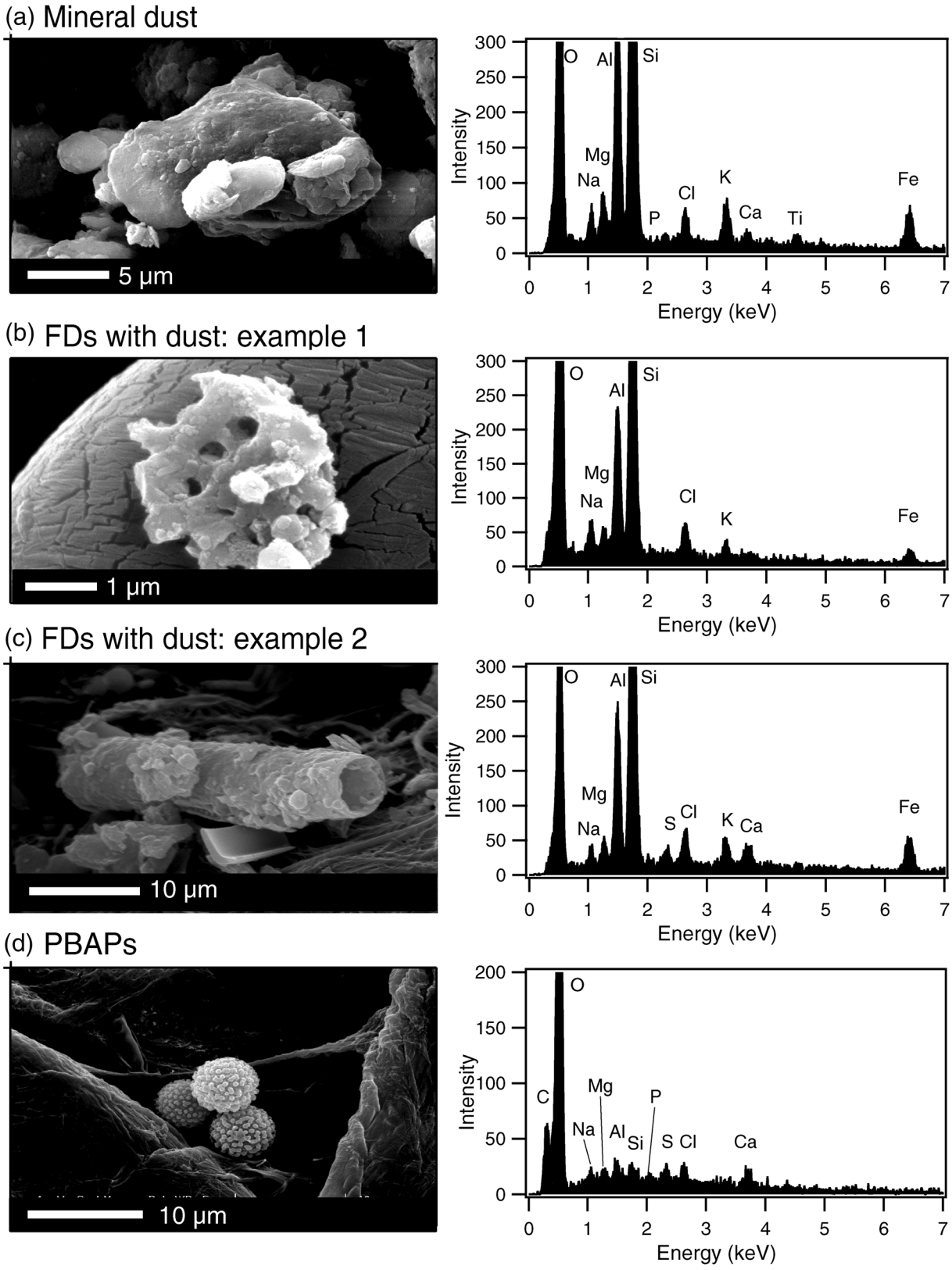

Figure 1. Representative scanning electron microscopy (SEM) images showing particle types (left) and energy dispersive X-ray spectroscopy (EDX) spectra (right) of each particle type: (a) mineral dust; (b) and (c) freshwater diatoms (FDs) internally mixed with dust; (d) primary biological aerosol particles (PBAPs). A cellulose filter fiber is shown behind the particle in (b). The field-of-view images corresponding to the particle spectra are shown in Figure S3.

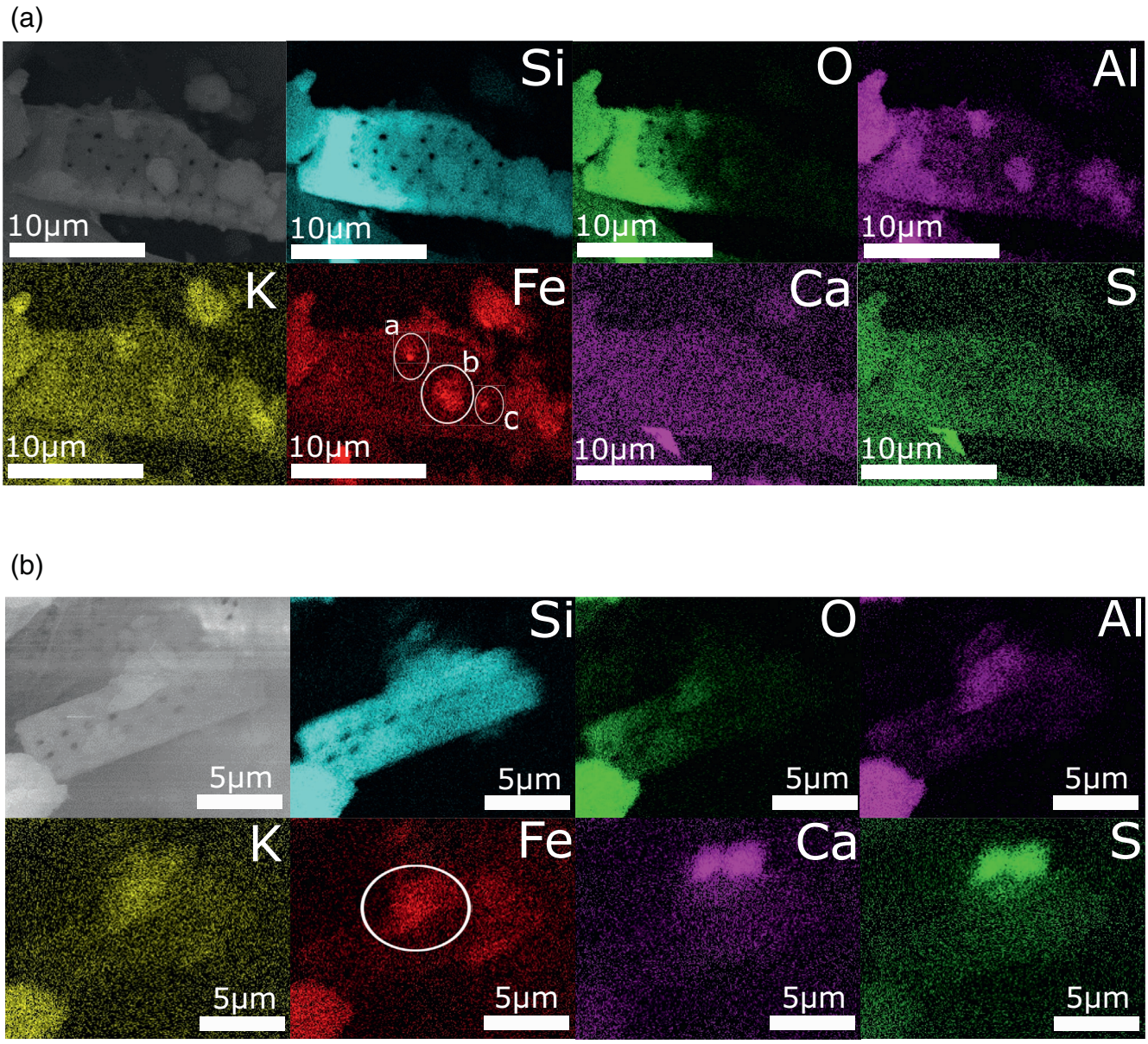

Figure 2. Panels (a and b) show two examples of scanning electron microscopy (SEM) images and corresponding energy dispersive X-ray spectroscopy (EDX) elemental maps of silicon (Si), oxygen (O), aluminum (Al), potassium (K), iron (Fe), calcium (Ca), and sulfur (S) on representative "FDs with dust." Increased brightness indicates more of the element. The white circles emphasize the Fe-containing dust inclusions.

collected within the Amazon Basin has also shown similar internal mixtures of dust and sea salt (Adachi et al., 2020; Artaxo & Hansson, 1995; Formenti et al., 2003; Fraund et al., 2017; Worobiec et al., 2007).

In this study, we also include a new class of particles transported to South America: FDs derived from African paleolakes internally mixed with dust (hereafter "FDs with dust"), which were identified primarily by morphology. FDs with dust comprised 3.5% of all particles and were identified by their regular pattern of holes characteristic of their frustules or by their tubular shape (Figure 1b and 1c). Because these particles were internally mixed with mineral dust, their composition as detected by EDX was similar to that of mineral dust. We excluded a marine source for these diatoms for the following reasons: (i) greater than 95% of the FD particles were internally mixed with dust including dust inclusions on the interior of the diatom frustule that would not be expected if dust were simply deposited on the diatoms during sample collection (see Figure S4 and S5 for examples), (ii) FDs were not present during nondust transport days, and (iii) FD

species in our Cayenne samples match those collected in sediment traps in the Atlantic Ocean near the coast of Africa (Gasse et al., 1989; Romero et al., 2003), Barbados (Reid, 2003), and the Bodélé Depression (Bristow et al., 2009) (see Figure S6 for SEM images of diatomite from the Bodélé Depression). FD species in our samples include *Aulacoseira granulate*, which was the most common FD found in our samples, *Stephanodiscus rotula*, *Hantzschia amphioxys*, and the genus *Cylotella*.

The detected FDs in our samples are thought to originate from African paleolakes (Bakker et al., 2019; Ben-Ami et al., 2010; Prospero et al., 2002; Washington & Todd, 2005). Soil from paleolakes is comprised of diatomite, a mixture of low density FDs (0.8 g cm^{-3}) and higher density authigenic minerals (2.7 g cm^{-3}) (Bristow et al., 2010; Conrad & Lappartient, 1991). FDs have been collected in Caribbean aerosols (Reid, 2003) and in open-ocean sediment cores in the NAO, which have been used to assess changes in the aridity of the Sahara (Gasse et al., 1989; Pokras & Mix, 1987; Skonieczny et al., 2019). However, to our knowledge, our work is the first to show the transport of diatomite from African paleolakes to South America. Previous studies have suggested that multiple paleolakes within the Sahara including the Bodélé Depression and other paleolakes in the western Sahara are active dust sources that can transport mineral aerosols to South America (Bakker et al., 2019; Prospero et al., 2002). These paleolakes could explain the detection of FDs in our samples. However, a recent study by Yu et al. (2020) suggests that dust from the Bodélé Depression is not transported to South America as frequently as previously thought, and that FDs internally mixed with dust may originate from other African sources (Bozlaker et al., 2018; Jewell et al., 2020; Kumar et al., 2014; Pourmand et al., 2014). We are unable to definitively pinpoint sources in this work without further geochemical analysis.

The remaining particles (1%) were classified as long-range transported PBAPs (Figure 1d). While these particles were not found in great abundance, previous research has shown that PBAPs are important to the global aerosol budgets (Artaxo et al., 1998; Mahowald et al., 2008; Pöschl et al., 2010). They were either spherical or ellipsoidal, which distinguished them from dust particles. They were composed primarily of carbon (C) and O along with trace amounts of phosphorus (P), potassium (K), sulfur (S), Ca, Na, and Cl—a composition similar to previously measured PBAPs in the Amazon (China et al., 2018; Graham et al., 2003; Wu et al., 2019).

3.2. Elemental Mapping of Fe-Containing Particles and Their Mixing State

Fe was associated with all particle types except PBAPs (Figure 1). Of the particles characterized as dust, 85% of particles contained Fe, a result similar to a previous study (Falkovich et al., 2001). Dust particles contained an average of 12% Fe by weight while FDs with dust contained an average of 4% Fe by weight with Fe abundance scaling with the size and amount of dust inclusions. Figure S7 further highlights this point.

To characterize Fe-rich dust inclusions on FD particles, we performed elemental mapping, which shows the spatial distribution of individual elements based on the characteristic X-rays emitted by different elements. Figure 2 shows two examples of SEM images of FDs with dust in the top left panel and associated elemental maps in the other panels. Additional elemental maps are shown in Figure S8. As expected, the Si and O maps outline the silicate frustule structure of the FD. The map of Al in Figure 2a shows that the FD itself does not contain any Al; rather, dust inclusions associated with the FDs contain Al. Fe is also associated with the dust inclusions attached to the surface of the FDs similar to previous work that has shown surficial Fe oxides on larger, transported dust particles (Lafon et al., 2006; Moskowitz et al., 2016). Fe-containing dust inclusions on FDs were measured, and the longest axis is reported as their diameter. In Figure 2a, there are three Fe-rich dust inclusions labeled a–c; the Fe inclusion in (a) is <0.1 μm in diameter; 2.6 μm in (b); and 1.5 μm in (c). Figure 2b shows a larger Fe inclusion with a diameter of 4.1 μm. These Fe-rich inclusions are smaller than the FDs that they are internally mixed with and are mainly found on the particle surface, which increases their susceptibility to chemical reactions, photoreduction, ligand complexation, and dissolution that can enhance Fe solubility (Baker & Jickells, 2006; Cwiertny et al., 2008; McDaniel et al., 2019; Paris & Desboeufs, 2013; Shi et al., 2011; Zhu et al., 1997).

In addition to Si, O, Al, and Fe, we also performed elemental mapping for S, Ca, and K. As shown in Figure 2, we observed only small amounts of S on dust suggesting limited reactions of supermicron dust with

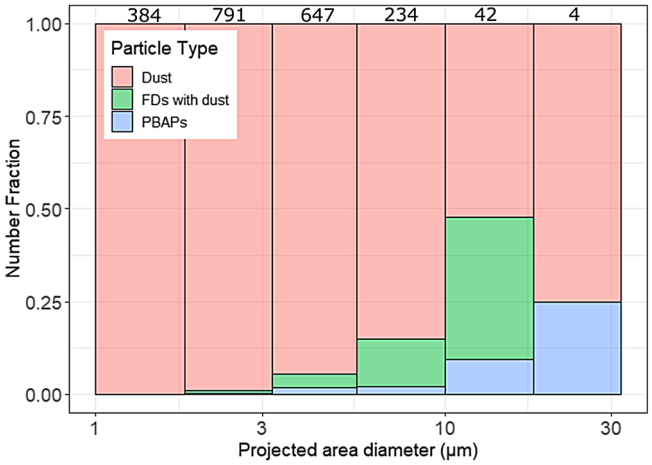

Figure 3. Relative fraction of each particle type: Dust (pink), Freshwater Diatoms (FDs) with dust (green), and Primary Biological Aerosol Particles (PBAPs; blue) as a function of projected area diameter (d_{pa}). The numbers in grey at the top show the number of particles in each size bin. Size bins are equally spaced on a log normal distribution with 4 bins per decade: 1.0–1.8, 1.8–3.2, 3.2–5.6, 5.6–10, 10–18, and 18–32 μm.

S-containing compounds typically found in the MBL, such as sulfuric acid or methanesulfonic acid. EDX analysis revealed that 16% of particles contained S, which is a lower fraction than observed in the central Amazon Basin (Wu et al., 2019). However, our observations are consistent with summertime dust measurements in marine and island environments (Denjean et al., 2016a; Kandler et al., 2018). In the central Amazon, there are more sources and emissions of S-containing species (e.g., SO_2 from pollution and biogenic sources) (Andreae et al., 1990; Wu et al., 2019). Therefore, we suggest that dust particles containing S-compounds observed in the central Amazon mainly underwent chemical reactions during transit from the coast to the interior of the Amazon, a distance on the order of 1,000 km. Elemental mapping results show that Ca and S are located in the same position on the dust particles (Figure 2a and 2b), indicating that S is associated with Ca, most likely in the form of gypsum ($CaSO_4 \cdot 2H_2O$). Gypsum could be a product of the chemical reaction of sulfur dioxide (SO_2) on the surface of calcite minerals (Andreae et al., 1986; Glaccum & Prospero, 1980; Ma et al., 2013) and reactions between calcite and sulfate from sea spray that occur in the atmosphere or subsequently after capture on the filter (Glaccum & Prospero, 1980). Other studies of long-range transported African dust using coupled SEM-EDX analysis also show gypsum from continental soil minerals (Coz et al., 2009; Falkovich et al., 2001), which could also explain our observations.

Elemental mapping also shows the presence of K on FDs and dust inclusions (Figure 2). From EDX spectra, K was found in about 62% of all mineral dust particles and was likely associated with K-feldspar minerals (Rizzolo et al., 2017; Scheuvens et al., 2013). It is possible that some of the K is due to the co-transport of biomass burning (Ansmann et al., 2009). Coagulation of biomass burning and dust has been observed over Africa and has been suggested to enhance the bioavailability of Fe associated with dust (Paris & Desboeufs, 2013;Paris et al., 2010). We did not observe any visual evidence of the coagulation of dust with biomass burning, a result similar to Kandler et al. (2011); however, we suggest additional measurements to further probe the presence of internally mixed biomass burning and dust in transported particles.

3.3. Particle Size Distributions and Asphericity

The relative number fraction of each particle type as a function of size is shown in Figure 3. Raw counts as a function of d_{pa} are shown in Figure S9. Mineral dust dominates each size bin in the supermicron fraction and accounts for an average of 98% of particles, by number, in the three smallest size bins (1.0–5.6 μm), which is within the range of previous studies of long-range transported African dust measured in the Caribbean (Denjean et al., 2016b; Maring et al., 2003; Reid, 2003) and the Amazon (Artaxo et al., 1998; Moran-Zuloaga et al., 2018). FDs with dust and PBAPs comprise an increasing fraction by number at larger sizes, including supercoarse mode particles ($d_{pa} > 10$ μm). FDs with dust accounted for 38% of all supercoarse mode particles analyzed from 10 to 18 μm and the sizes of FDs with dust were significantly larger than dust (p value < 0.005). The d_{pa} of PBAPs ranged from 2.4 to 19 μm, which is similar to previous measurements of PBAPs in the Amazon (Graham et al., 2003; Worobiec et al., 2007). Overall, FDs and PBAPs comprised nearly 50% of supercoarse mode particles by number between 10 and 18 μm in diameter.

We also measured the aspect ratio (AR_{perp}) of particles transported to Cayenne (Figure 4 and Table S1) using a subset of particles. An increasing value of AR_{perp} indicates increased particle asphericity while a value of one indicates a spherical particle. Figure 4 shows that for all particle types, average AR_{perp} increases with increasing particle size, which is in agreement with other field studies of transported African dust (Kandler et al., 2011; Ryder et al., 2018; Saxby et al., 2018). The average AR_{perp} of all dust particles is 1.6, which is similar to previously reported values of AR_{perp} for boreal summertime long-range transported African dust (Huang et al., 2020). Interestingly, the average AR_{perp} of all FDs with dust was 2.5, significantly larger than

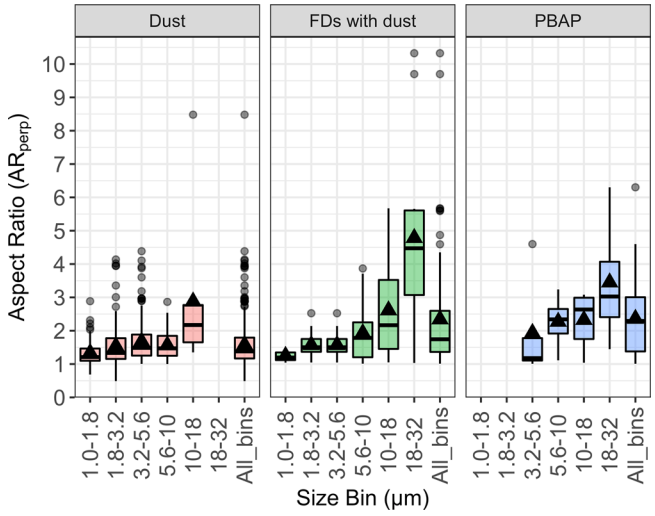

Figure 4. Aspect ratios (AR_{perp}) for dust (pink), FDs with dust (green), and PBAPs (blue). The center horizontal line of the box and whisker plot shows the median and the colored area shows the interquartile range. Whiskers show minimum and maximum values with grey dots representing outliers. The black triangles represent the mean of the data in each size bin. "All_bins" represents the AR across all size bins for each particle type. Gaps in the data represent either no particles or only one particle in the size bin. Note that the x axis is plotted as d_{max}.

pure dust particles (p value < 0.005), which is likely due to their tubular shapes (Figure 1c). Additionally, the median AR_{perp} of just the supercoarse mode FDs with dust was 3.7 with median values up to AR_{perp} of almost five clearly showing the increase in asphericity with particle size. PBAPs had an average AR_{perp} of 2.2. The elevated AR_{perp} and asphericity observed for all particle types that increase with particle diameter may explain the surprising long-range transport of supercoarse mode particles from Africa to the coast of French Guiana.

4. Conclusions and Atmospheric Implications

Our research highlights the diversity of Fe-containing particles transported to South America, including supercoarse mode particles, and serves as an important stepping-stone toward understanding the potential significance of these particles for marine biogeochemical cycles. Because most biogeochemistry models assume that supercoarse mode particles deposit close to their sources (Mahowald et al., 2014; Myriokefalitakis et al., 2018), our work sought to elucidate potential mechanisms that could explain large particle transport to our site. First, we found that particle asphericity (AR_{perp}) increases as a function of particle diameter, suggesting that particle shape reduces the settling velocity of large particles, particularly for unfragmented FDs whose tubular structure is still intact. The low density of FDs also enhances their atmospheric lifetime. Assuming FDs with dust represent a 1:1 mixture of FDs and dust, FDs with dust would have a 35% slower settling velocity when compared to similarly sized dust particles (Huang et al., 2020).

The same physical properties that decrease the atmospheric settling velocity for FDs with dust likely also decrease their sinking velocity in the water column. We estimate that FDs with dust have a 79% slower sinking velocity in surface water compared to dust based on particle shape, aspect ratio, and density (McDonnell & Buesseler, 2010). Details of these calculations are in the SI. A slower sinking velocity in the water column would enhance the residence time of FDs in surface waters compared to dust and increase the timescale for dissolution of the surficial Fe-rich inclusions that were observed on these particles. Additionally, a slower sinking velocity could increase the ability of FDs with dust to be carried by surface currents, increasing the spatial impact of FDs with dust.

In this study, we suggest that the transport of FDs with dust may facilitate delivery of Fe to remote marine ecosystems because of their low settling velocities in air and seawater. Even though FDs with dust accounted for 3.5% of the total particles analyzed by number fraction, they are consistently as large or larger than dust particles and comprise 38% of supercoarse mode particles by number between 10 and 18 μm, contain Fe-rich dust inclusions that extend Fe-containing dust into the supercoarse mode, and contain an average of 4% Fe by weight suggesting their potential impact on marine biogeochemical cycles. FDs found in open-ocean sediment cores in the NAO have also been linked to an increase in African aridity (Gasse et al., 1989; Pokras & Mix, 1987). Based on our results in present-day samples of FDs internally mixed with dust, FDs with dust could also have been a source of Fe to the equatorial NAO during previous climate regimes. We suggest additional studies that better quantify the contribution of FDs to the transported aerosol burden including both the wet and dry deposition rates of these particles to determine whether diatoms are indeed preferentially transported across the equatorial NAO during the dust transport season.

Data Availability Statement

Datasets in this study are available at the University of Miami's Data Repository (under DOI https://doi.org/10.17604/jmtk-yb12).

Acknowledgments
We thank ATMO-Guyane for collecting samples in Cayenne, French Guiana (https://www.atmo-guyane.org/). The authors acknowledge the NOAA Air Resources Laboratory (ARL) for the provision of the HYSPLIT transport and dispersion model and READY website (https://www.ready.noaa.gov/HYSPLIT.php). Cassandra J. Gaston acknowledges funding provided by the Provost Award from the University of Miami and an NSF CAREER award (AGS-1944958). Some microscopy analyses were performed at the Environmental Molecular Sciences Laboratory (user proposal #50816), a national scientific user facility located at the Pacific Northwest National Laboratory and sponsored by the Office of Biological and Environmental Research of the U.S. Department of Energy. The authors acknowledge the Michigan Center for Materials Characterization (MC^2) for use of the instruments and staff assistance. We thank Johann Engelbrecht (Desert Research Institute) for the sample from the Bodélé Depression as well as the two anonymous reviewers whose suggestions greatly improved this manuscript.

References

Adachi, K., Oshima, N., Gong, Z., de Sá, S., Bateman, A. P., Martin, S. T., et al. (2020). Mixing states of Amazon basin aerosol particles transported over long distances using transmission electron microscopy. *Atmospheric Chemistry and Physics*, *20*(20), 11923–11939. https://doi.org/10.5194/acp-20-11923-2020

Adebiyi, A. A., & Kok, J. F. (2020). Climate models miss most of the coarse dust in the atmosphere. *Science Advances*, *6*(15), eaaz9507. https://doi.org/10.1126/sciadv.aaz9507

Andreae, M. O., Berresheim, H., Bingemer, H., Jacob, D. J., Lewis, B. L., Li, S. M., & Talbot, R. W. (1990). The atmospheric sulfur cycle over the Amazon Basin. 2. Wet season. *Journal of Geophysical Research*, *95*(D10), 16813–16824.

Andreae, M. O., Charlson, R. J., Bruynseels, F., Storms, H., Van Grieken, R., & Maenhaut, W. (1986). Internal mixture of sea salt, silicates, and excess sulfate in marine aerosols. *Science*, *232*, 1620–1623. https://doi.org/10.1210/jcem-10-10-1361

Ansmann, A., Baars, H., Tesche, M., Müller, D., Althausen, D., Engelmann, R., et al. (2009). Dust and smoke transport from Africa to South America: Lidar profiling over Cape Verde and the Amazon rainforest. *Geophysical Research Letters*, *36*, L11802. https://doi.org/10.1029/2009GL037923

Artaxo, P., Fernandes, E., Martins, J., Yamasoe, M., Hobbs, P., Maenhaut, W., et al. (1998). Large-scale aerosol source apportionment in Amazonia. *Journal of Geophysical Research*, *103*(D24), 31837–31847.

Artaxo, P., & Hansson, H. C. (1995). Size distribution of biogenic aerosol particles from the amazon basin. *Atmospheric Environment*, *29*(3), 393–402. https://doi.org/10.1016/1352-2310(94)00178-N

Artaxo, P., Storms, H., Bruynseels, F., Van Grieken, R., & Maenhaut, W. (1988). Composition and sources of aerosols from the Amazon Basin. *Journal of Geophysical Research*, *93*(D2), 1605–1615.

Baker, A. R., & Jickells, T. D. (2006). Mineral particle size as a control on aerosol iron solubility. *Geophysical Research Letters*, *33*, L17608. https://doi.org/10.1029/2006GL026557

Bakker, N. L., Drake, N. A., & Bristow, C. S. (2019). Evaluating the relative importance of Northern African mineral dust sources using remote sensing. *Atmospheric Chemistry and Physics*, *19*, 10525–10535. https://doi.org/10.5194/acp-2019-253

Barkley, A. E., Prospero, J. M., Mahowald, N., Hamilton, D. S., Popendorf, K. J., Oehlert, A. M., et al. (2019). African biomass burning is a substantial source of phosphorus deposition to the Amazon, Tropical Atlantic Ocean, and Southern Ocean. *Proceeding of the National Academy of Sciences of the United States of America*, *116*(33), 16216–16221. https://doi.org/10.1073/pnas.1906091116

Ben-Ami, Y., Koren, I., Rudich, Y., Artaxo, P., Martin, S. T., & Andreae, M. O. (2010). Transport of North African dust from the Bodélé depression to the Amazon Basin: A case study. *Atmospheric Chemistry and Physics*, *10*(16), 7533–7544. https://doi.org/10.5194/acp-10-7533-2010

Betzer, P. R., Carder, K. L., Duce, R. A., Merrill, J. T., Tindale, N. W., Uematsu, M., et al. (1988). Long-range transport of giant mineral aerosol particles. *Nature*, *336*, 403–405. https://doi.org/10.1038/332141a0

Bozlaker, A., Prospero, J. M., Price, J., & Chellam, S. (2018). Linking Barbados mineral dust aerosols to North African sources using elemental composition and radiogenic Sr, Nd, and Pb isotope signatures. *Journal of Geophysical Research: Atmospheres*, *123*, 1384–1400. https://doi.org/10.1002/2017JD027505

Bristow, C. S., Drake, N., & Armitage, S. (2009). Deflation in the dustiest place on Earth: The Bodélé Depression, Chad. *Geomorphology*, *105*(1–2), 50–58. https://doi.org/10.1016/j.geomorph.2007.12.014

Bristow, C. S., Hudson-Edwards, K. A., & Chappell, A. (2010). Fertilizing the Amazon and equatorial Atlantic with West African dust. *Geophysical Research Letters*, *37*, L14807. https://doi.org/10.1029/2010GL043486

Buck, C. S., Landing, W. M., Resing, J. A., & Measures, C. I. (2010). The solubility and deposition of aerosol Fe and other trace elements in the North Atlantic Ocean: Observations from the A16N CLIVAR/CO2repeat hydrography section. *Marine Chemistry*, *120*(1–4), 57–70. https://doi.org/10.1016/j.marchem.2008.08.003

Carlson, T., & Prospero, J. M. (1972). The large-scale movement of Saharan air outbreaks over the Northern Equatorial Atlantic, *Journal of Applied Meteorology*, *11*(2), 283–297.

Chiapello, I., Bergametti, G., Gomes, L., Chatenet, B., Dulac, F., Pimenta, J., & Suares, E. S. (1995). An additional low layer transport of Sahelian and Saharan dust over the north-eastern Tropical Atlantic. *Geophysical Research Letters*, *22*(23), 3191–3194.

China, S., Burrows, S. M., Wang, B., Harder, T. H., Weis, J., Tanarhte, M., et al. (2018). Fungal spores as a source of sodium salt particles in the Amazon basin. *Nature Communications*, *9*(1), 4793. https://doi.org/10.1038/s41467-018-07066-4

Conrad, G., & Lappartient, J. R. (1991). The appearance of Cardium fauna and foraminifers in the great lakes of the early quaternary period in the Algerian central Sahara desert. *Journal of African Earth Sciences*, *12*(1–2), 375–382. https://doi.org/10.1016/0899-5362(91)90086-E

Coz, E., Gómez-Moreno, F. J., Pujadas, M., Casuccio, G. S., Lersch, T. L., & Artíñano, B. (2009). Individual particle characteristics of North African dust under different long-range transport scenarios. *Atmospheric Environment*, *43*(11), 1850–1863. https://doi.org/10.1016/j.atmosenv.2008.12.045

Cwiertny, D. M., Baltrusaitis, J., Hunter, G. J., Laskin, A., Scherer, M. M., & Grassian, V. H. (2008). Characterization and acid-mobilization study of iron-containing mineral dust source materials. *Journal of Geophysical Research*, *113*, D05202. https://doi.org/10.1029/2007JD009332

Denjean, C., Caquineau, S., Desboeufs, K., Laurent, B., Maille, M., Quiñones, M., et al. (2016). Long-range transport across the Atlantic in summertime does not enhance the hygroscopicity of African mineral dust. *Geophysical Research Letters*, *31*, 7835–7843. https://doi.org/10.1002/2015GL065693

Denjean, C., Formenti, P., Desboeufs, K., Chevaillier, S., Triquet, S., Maillé, M., et al. (2016). Size distribution and optical properties of African mineral dust after intercontinental transport. *Journal of Geophysical Research: Atmospheres*, *121*, 7117–7138. https://doi.org/10.1002/2016JD024783

Falkovich, A. H., Ganor, E., Levin, Z., Formenti, P., & Rudich, Y. (2001). Chemical and mineralogical analysis of individual mineral dust particles. *Journal of Geophysical Research*, *106*(D16), 18029–18036.

Formenti, P., Elbert, W., Maenhaut, W., Haywood, J., & Andreae, M. O. (2003). Chemical composition of mineral dust aerosol during the Saharan Dust Experiment (SHADE) airborne campaign in the Cape Verde region, September 2000. *Journal of Geophysical Research*, *108*(D18), 8576. https://doi.org/10.1029/2002JD002648

Fraund, M., Pham, D. Q., Bonanno, D., Harder, T. H., Wang, B., Brito, J.,et al. (2017). Elemental mixing state of aerosol particles collected in Central Amazonia during GoAmazon2014/15. *Atmosphere (Basel)*, *8*(9), 173. https://doi.org/10.3390/atmos8090173

Gasse, F., Stabell, B., Fourtanier, E., & van Iperen, Y. (1989). Freshwater diatom influx in intertropical Atlantic: Relationships with continental records from Africa. *Quaternary Research*, *32*(2), 229–243. https://doi.org/10.1016/0033-5894(89)90079-3

Gaston, C. J. (2020). Re-examining dust chemical aging and its impacts on Earth's climate. *Accounts of Chemical Research*, *53*(5), 1005–1013. https://doi.org/10.1021/acs.accounts.0c00102

Glaccum, R. A., & Prospero, J. M. (1980). Saharan aerosols over the tropical north Atlantic—Mineralogy. *Marine Geology*, *37*, 295–321.

Graham, B., Guyon, P., Maenhaut, W., Taylor, P. E., Ebert, M., Matthias-Maser, S., et al. (2003). Composition and diurnal variability of the natural Amazonian aerosol. *Journal of Geophysical Research*, *108*(D24), 4765. https://doi.org/10.1029/2003JD004049

Hamilton, D. S., Moore, J. K., Arneth, A., Bond, T. C., Carslaw, K. S., Hantson, S., et al. (2020). Impact of changes to the atmospheric soluble iron deposition flux on ocean biogeochemical cycles in the anthropocene. *Global Biogeochemical Cycles*, *34*(3), 1–22. https://doi.org/10.1029/2019GB006448

Huang, Y., Kok, J. F., Kandler, K., Lindqvist, H., Nousiainen, T., Sakai, T., et al. (2020). Climate models and remote sensing retrievals neglect substantial desert dust asphericity. *Geophysical Research Letters*, *47*, e2019GL086592. https://doi.org/10.1029/2019GL086592

Ingall, E. D., Feng, Y., Longo, A. F., Lai, B., Shelley, R. U., Landing, W. M., et al. (2018) Enhanced iron solubility at low pH in global aerosols. *Atmosphere (Basel)*, *9*(5), 1–17. https://doi.org/10.3390/ATMOS9050201

Ito, A., Myriokefalitakis, S., Kanakidou, M., Mahowald, N. M., Scanza, R. A., Hamilton, D. S., et al. (2019). Pyrogenic iron: The missing link to high iron solubility in aerosols. *Science Advances*, *5*(5), 13–15. https://doi.org/10.1126/sciadv.aau7671

Jewell, A. M., Drake, N., Crocker, A. J., Bakker, N. L., Kunkelova, T., Bristow, C. S., et al. (2020). Three North African dust source areas and their geochemical fingerprint. *Earth and Planetary Science Letters*, *1*, 116645. https://doi.org/10.1016/j.epsl.2020.116645

Jickells, T. D., & Moore, C. M. (2015). The importance of atmospheric deposition for ocean productivity. *Annual Review of Ecology, Evolution, and Systematics*, *46*, 481–501.

Journet, E., Desboeufs, K. V, Caquineau, S., & Colin, J. (2008). Mineralogy as a critical factor of dust iron solubility. *Geophysical Research Letters*, *35*, L07805. https://doi.org/10.1029/2007GL031589

Kandler, K., Lieke, K., Benker, N., Emmel, C., Küpper, M., Müller-Ebert, D., et al. (2011). Electron microscopy of particles collected at Praia, Cape Verde, during the Saharan Mineral Dust Experiment: Particle chemistry, shape, mixing state and complex refractive index. *Tellus B: Chemical and Physical Meteorology*, *63*(4), 475–496. https://doi.org/10.1111/j.1600-0889.2011.00550.x

Kandler, K., Schneiders, K., Ebert, M., Hartmann, M., Weinbruch, S., Prass, M., & Pöhlker, C. (2018). Composition and mixing state of atmospheric aerosols determined by electron microscopy: Method development and application to aged Saharan dust deposition in the Caribbean boundary layer. *Atmospheric Chemistry and Physics*, *18*(18), 13429–13455. https://doi.org/10.5194/acp-18-13429-2018

Kok, J. F., Ridley, D. A., Zhou, Q., Miller, R. L., Zhao, C., Heald, C. L., et al. (2017). Smaller desert dust cooling effect estimated from analysis of dust size and abundance. *Nature Geoscience*, *10*(4), 274–278. https://doi.org/10.1038/ngeo2912

Kumar, A., Abouchami, W., Galer, S. J. G., Garrison, V. H., Williams, E., & Andreae, M. O. (2014). A radiogenic isotope tracer study of transatlantic dust transport from Africa to the Caribbean. *Atmospheric Environment*, *82*, 130–143. https://doi.org/10.1016/j.atmosenv.2013.10.021

Lafon, S., Sokolik, I. N., Rajot, J. L., Caquincau, S., & Gaudichet, A. (2006). Characterization of iron oxides in mineral dust aerosols: Implications for light absorption. *Journal of Geophysical Research*, *111*, D21207. https://doi.org/10.1029/2005JD007016

Ma, Q., He, H., Liu, Y., Liu, C., & Grassian, V. H. (2013). Heterogeneous and multiphase formation pathways of gypsum in the atmosphere. *Physical Chemistry Chemical Physics*, *15*(44), 19196–19204. https://doi.org/10.1039/c3cp53424c

Mahowald, N. (2011). Aerosol indirect effect on biogeochemical cycles and climate. *Science*, *334*(6057), 794–796.

Mahowald, N., Albani, S., Kok, J. F., Engelstaeder, S., Scanza, R., Ward, D. S., & Flanner, M. G. (2014). The size distribution of desert dust aerosols and its impact on the Earth system. *Aeolian Research*, *15*, 53–71. https://doi.org/10.1016/j.aeolia.2013.09.002

Mahowald, N., Jickells, T. D., Baker, A. R., Artaxo, P., Benitez-Nelson, C. R., Bergametti, G., et al. (2008). Global distribution of atmospheric phosphorus sources, concentrations and deposition rates, and anthropogenic impacts. *Global Biogeochemical Cycles*, *22*, GB4026. https://doi.org/10.1029/2008GB003240

Mahowald, N. M., Baker, A. R., Bergametti, G., Brooks, N., Duce, R. A., Jickells, T. D., et al. (2005). Atmospheric global dust cycle and iron inputs to the ocean. *Global Biogeochemical Cycles*, *19*, GB4025. https://doi.org/10.1029/2004GB002402

Mallios, S. A., Drakaki, E., & Amiridis, V. (2020). Effects of dust particle sphericity and orientation on their gravitational settling in the earth's atmosphere. *Journal of Aerosol Science*, *150*, 105634. https://doi.org/10.1016/j.jaerosci.2020.105634

Maring, H., Savoie, D. L., Izaguirre, M. A., Custals, L., & Reid, J. S. (2003). Mineral dust aerosol size distribution change during atmospheric transport. *Journal of Geophysical Research*, *108*(D19), 8592. https://doi.org/10.1029/2002JD002536

McDaniel, M. F. M., Ingall, E. D., Morton, P. L., Castorina, E., Weber, R. J., Shelley, R. U., et al. (2019). Relationship between atmospheric aerosol mineral surface area and iron solubility. *ACS Earth and Space Chemistry*, *3*(11), 2443–2451. https://doi.org/10.1021/acsearthspacechem.9b00152

McDonnell, A. M. P., & Buesseler, K. O. (2010). Variability in the average sinking velocity of marine particles. *Limnology and Oceanography*, *55*(5), 2085–2096. https://doi.org/10.4319/lo.2010.55.5.2085

Mills, M. M., Ridame, C., Davey, M., La Roche, J., & Geider, R. J. (2004). Iron and phosphorus co-limit nitrogen fixation in the eastern tropical North Atlantic. *Nature*, *429*, 292–294.

Moore, C. M., Mills, M. M., Arrigo, K. R., Berman-Frank, I., Bopp, L., Boyd, P. W., et al. (2013). Processes and patterns of oceanic nutrient limitations, *Nature Geoscience*, *6*, 701–710, https://doi.org/10.1038/ngeo1765

Moran-Zuloaga, D., Ditas, F., Walter, D., Saturno, J., Brito, J., Carbone, S., et al. (2018). Long-term study on coarse mode aerosols in the Amazon rain forest with the frequent intrusion of Saharan dust plumes. *Atmospheric Chemistry and Physics*, *18*(13), 10055–10088. https://doi.org/10.5194/acp-18-10055-2018

Moskowitz, B. M., Reynolds, R. L., Goldstein, H. L., Berquó, T. S., Kokaly, R. F., & Bristow, C. S. (2016). Iron oxide minerals in dust-source sediments from the Bodele Depression, Chad: Implications for radiative properties and Fe bioavailability of dust plumes from the Sahara. *Aeolian Research*, *22*, 93–106.

Myriokefalitakis, S., Ito, A., Kanakidou, M., Nenes, A., Krol, M. C., Mahowald, N. M., et al. (2018). Reviews and syntheses: The GESAMP atmospheric iron deposition model intercomparison study. *Biogeosciences*, *15*(21), 6659–6684. https://doi.org/10.5194/bg-15-6659-2018

Okin, G. S., Baker, A. R., Tegen, I., Mahowald, N. M., Dentener, F. J., Duce, R. A., et al. (2011). Impacts of atmospheric nutrient deposition on marine productivity: Roles of nitrogen, phosphorus, and iron. *Global Biogeochemical Cycles*, *25*, GB2022. https://doi.org/10.1029/2010GB003858

Paris, R., & Desboeufs, K. V (2013). Effect of atmospheric organic complexation on iron-bearing dust solubility. *Atmospheric Chemistry and Physics*, *13*, 4895–4905. https://doi.org/10.5194/acp-13-4895-2013

Paris, R., Desboeufs, K. V., Formenti, P., Nava, S., & Chou, C. (2010). Chemical characterisation of iron in dust and biomass burning aerosols during AMMA-SOP0/DABEX: Implication for iron solubility. *Atmospheric Chemistry and Physics*, *10*(9), 4273–4282. https://doi.org/10.5194/acp-10-4273-2010

Pokras, E. M., & Mix, A. C. (1987). Earth's precession cycle and Quaternary climatic change in tropical Africa. *Nature*, *326*(6112), 486–487. https://doi.org/10.1038/326486a0

Pöschl, U., Martin, S. T., Sinha, B., Chen, Q., Gunthe, S. S., Huffman, J. A., et al. (2010). Rainforest aerosols as biogenic nuclei of clouds and precipitation in the Amazon. *Science*, *329*(5998), 1513–1516.

Pourmand, A., Prospero, J. M., & Sharifi, A. (2014). Geochemical fingerprinting of trans-Atlantic African dust based on radiogenic Sr-Nd-Hf isotopes and rare earth element anomalies. *Geology*, *42*(8), 675–678. https://doi.org/10.1130/G35624.1

Prospero, J. M., Barkley, A. E., Gaston, C. J., Gatineau, A., Campos y Sansano, A., & Panechou, K. (2020). Characterizing and quantifying African dust transport and deposition to South America: Implications for the phosphorus budget in the Amazon Basin. *Global Biogeochemical Cycles*, *34*, e2020GB006536. https://doi.org/10.1029/2020GB006536

Prospero, J. M., Bonatti, E., Schubert, C., & Carlson, T. (1970). Dust in the Caribbean atmosphere traced to an African dust storm. *Earth and Planetary Science Letters*, *9*, 287–293.

Prospero, J. M., Glaccum, R. A., & Nees, R. T. (1981). Atmospheric transport of soil dust from Africa to South America. *Nature*, *289*, 570–572.

Prospero, J. M., Ginoux, P., Torres, O., Nicholson, S. E., & Gill, T. E. (2002). Environmental characterization of global sources of atmospheric soil dust identified with the Nimbus 7 Total Ozone Mapping Spectrometer (TOMS) absorbing aerosol product. *Reviews of Geophysics*, *40*(1), 1002. https://doi.org/10.1029/2000RG000095

Reid, E. A. (2003). Characterization of African dust transported to Puerto Rico by individual particle and size segregated bulk analysis. *Journal of Geophysical Research*, *108*(D19), 8591. https://doi.org/10.1029/2002JD002935

Rizzolo, J. A., Barbosa, C. G. G., Borillo, G. C., Godoi, A. F. L., Souza, R. A. F., Andreoli, R. V., et al. (2017). Soluble iron nutrients in Saharan dust over the central Amazon rainforest. *Atmospheric Chemistry and Physics*, *17*(4), 2673–2687. https://doi.org/10.5194/acp-17-2673-2017

Rolph, G., Stein, A., & Stunder, B. (2017). Real-time Environmental Applications and Display sYstem: READY. *Environmental Modelling Software*, *95*, 210–228.

Romero, O. E., Dupont, L., Wyputta, U., Jahns, S., & Wefer, G. (2003). Temporal variability of fluxes of eolian-transported freshwater diatoms, phytoliths, and pollen grains off Cape Blanc as reflection of land-atmosphere-ocean interactions in northwest Africa. *Journal of Geophysical Research*, *108*(C5), 3153. https://doi.org/10.1029/2000JC000375

Ryder, C. L., Highwood, E. J., Walser, A., Seibert, P., Philipp, A., & Weinzierl, B. (2019). Coarse and giant particles are ubiquitous in Saharan dust export regions and are radiatively significant over the Sahara. *Atmospheric Chemistry and Physics*, *19*(24), 15353–15376. https://doi.org/10.5194/acp-19-15353-2019

Ryder, C. L., Marenco, F., Brooke, J. K., Estelles, V., Cotton, R., Formenti, P., et al. (2018). Coarse-mode mineral dust size distributions, composition and optical properties from AER-D aircraft measurements over the tropical eastern Atlantic. *Atmospheric Chemistry and Physics*, *18*(23), 17225–17257. https://doi.org/10.5194/acp-18-17225-2018

Saxby, J., Beckett, F., Cashman, K., Rust, A., & Tennant, E. (2018). The impact of particle shape on fall velocity: Implications for volcanic ash dispersion modelling. *Journal of Volcanology Geothermal Research*, *362*, 32–48. https://doi.org/10.1016/j.jvolgeores.2018.08.006

Scheuvens, D., Schütz, L., Kandler, K., Ebert, M., & Weinbruch, S. (2013). Bulk composition of northern African dust and its source sediments—A compilation. *Earth-Science Reviews*, *116*(1), 170–194. https://doi.org/10.1016/j.earscirev.2012.08.005

Shi, Z., Krom, M. D., Bonneville, S., Baker, A. R., Bristow, C., Drake, N., et al. (2011). Influence of chemical weathering and aging of iron oxides on the potential iron solubility of Saharan dust during simulated atmospheric processing. *Global Biogeochemical Cycles*, *25*, GB2010. https://doi.org/10.1029/2010GB003837

Shi, Z., Krom, M. D., Bonneville, S., Baker, A. R., Jickells, T. D., & Benning, L. G. (2009). Formation of iron nanoparticles and increase in iron reactivity in mineral dust during simulated cloud processing. *Environmental Science and Technology*, *43*(17), 6592–6596. https://doi.org/10.1021/es901294g

Skonieczny, C., McGee, D., Winckler, G., Bory, A., Bradtmiller, L. I., Kinsley, C. W., et al. (2019). Monsoon-driven Saharan dust variability over the past 240,000 years. *Science Advances*, *5*(1), 1–9. https://doi.org/10.1126/sciadv.aav1887

Spokes, L. J., & Jickells, T. D. (1995). Factors controlling the solubility of aerosol trace metals in the atmosphere and on mixing into seawater. *Aquatic Geochemistry*, *1*(4), 355–374. https://doi.org/10.1007/BF00702739

Stein, A. F., Draxler, R. R., Rolph, G. D., Stunder, B. J. B., Cohen, M. D., & Ngan, F. (2015). NOAA's HYSPLIT atmospheric transport and dispersion modeling system. *Bulletin of the American Meteorological Society*, *96*, 2059–2077.

Trapp, J. M., Millero, F. J., & Prospero, J. M. (2010). Trends in the solubility of iron in dust-dominated aerosols in the equatorial Atlantic trade winds: Importance of iron speciation and sources. *Geochemistry, Geophysics, Geosystems*, *11*, D05202. https://doi.org/10.1029/2009GC002651

Tsamalis, C., Chédin, A., Pelon, J., & Capelle, V. (2013). The seasonal vertical distribution of the Saharan Air Layer and its modulation by the wind. *Atmospheric Chemistry and Physics*, *13*, 11235–11257.

van der Does, M., Knippertz, P., Zschenderlein, P., Giles Harrison, R., & Stuut, J. B. W. (2018). The mysterious long-range transport of giant mineral dust particles. *Science Advances*, *4*(12), 1–9. https://doi.org/10.1126/sciadv.aau2768

van der Does, M., Korte, L. F., Munday, C. I., Brummer, G. J. A., & Stuut, J. B. W. (2016). Particle size traces modern Saharan dust transport and deposition across the equatorial North Atlantic. *Atmospheric Chemistry and Physics*, *16*(21), 13697–13710. https://doi.org/10.5194/acp-16-13697-2016

Wang, R., Balkanski, Y., Boucher, O., Ciais, P., Peñuelas, J., & Tao, S. (2015). Significant contribution of combustion-related emissions to the atmospheric phosphorus budget. *Nature Geoscience*, *8*(1), 48–54. https://doi.org/10.1038/ngeo2324

Washington, R., & Todd, M. C. (2005). Atmospheric controls on mineral dust emission from the Bodélé Depression, Chad: The role of the low level jet. *Geophysical Research Letters*, *32*, L17701. https://doi.org/10.1029/2005GL023597

Weinzierl, B., Ansmann, A., Prospero, J. M., Althausen, D., Benker, N., Chouza, F., et al (2017). The Saharan aerosol long-range transport and aerosol-cloud-interaction experiment: Overview and selected highlights. *Bulletin of the American Meteorological Society*, *98*(7), 1427–1451. https://doi.org/10.1175/BAMS-D-15-00142.1

Weinzierl, B., Petzold, A., Esselborn, M., Wirth, M., Rasp, K., Kandler, K., et al. (2009). Airborne measurements of dust layer properties, particle size distribution and mixing state of Saharan dust during SAMUM 2006. *Tellus B: Chemical and Physical Meteorology*, *61*(1), 96–117. https://doi.org/10.1111/j.1600-0889.2008.00392.x

Worobiec, A., Szalóki, I., Osán, J., Maenhaut, W., Anna Stefaniak, E., & Van Grieken, R. (2007). Characterisation of Amazon Basin aerosols at the individual particle level by X-ray microanalytical techniques. *Atmospheric Environment*, *41*(39), 9217–9230. https://doi.org/10.1016/j.atmosenv.2007.07.056

Wu, L., Li, X., Kim, H., Geng, H., Godoi, R. H. M., Barbosa, C. G. G., et al. (2019). Single-particle characterization of aerosols collected at a remote site in the Amazonian rainforest and an urban site in Manaus, Brazil. *Atmospheric Chemistry and Physics*, *19*(2), 1221–1240. https://doi.org/10.5194/acp-19-1221-2019

Yu, Y., Kalashnikova, O. V, Garay, M. J., Lee, H., & Notaro, M. (2020). Disproving the Bodélé depression as the primary source of dust fertilizing the Amazon Rainforest. *Geophysical Research Letters*, *47*, e2020GL088020. https://doi.org/10.1029/2020GL088020

Zhu, X. R., Prospero, J. M., & Millero, F. J. (1997). Diel variability of soluble Fe(II) and soluble total Fe in North Africa dust in the trade winds at Barbados. *Journal of Geophysical Research*, *102*(D17), 21297–21305.